

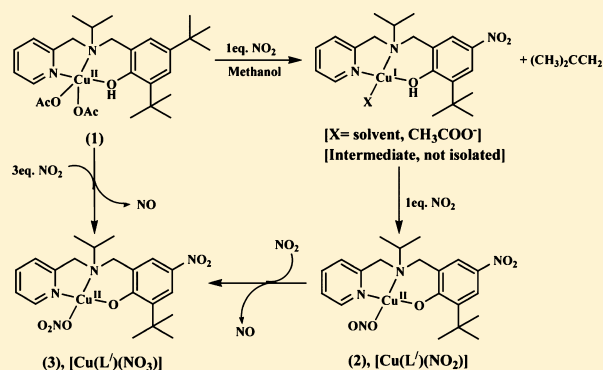
Oxo Transfer from Nitrogen Dioxide to Nitrito Group in a Copper(II) Complex

Kuldeep Gogoi, Hemanta Deka, Vikash Kumar, and Biplab Mondal*

Department of Chemistry, Indian Institute of Technology Guwahati, Guwahati, Assam 781039, India

Supporting Information

ABSTRACT: Reaction of Cu(II) complex $[\text{Cu}^{\text{II}}(\text{LH})(\text{O}_2\text{CCH}_3)_2]$ (1) [$\text{LH} = 4,6\text{-di-}t\text{-butyl-}2\text{-}((2\text{-picolyl(isopropyl)amino)methyl)\text{-phenol}]$] with equivalent amount of NO_2 leads to the reduction of Cu(II) to Cu(I) with concomitant nitration at the phenol ring of the ligand. This resulted in the in situ formation of intermediate Cu(I) complex of the nitrated ligand ($\text{L}'\text{H}$). Additional equivalent of NO_2 coordinates to the Cu(I) complex to form corresponding O-nitrito Cu(II) complex $[\text{Cu}^{\text{II}}(\text{L}'(\eta^1\text{-ONO}))]$ (2). Subsequent addition of NO_2 led to the corresponding O-nitrato complex, $[\text{Cu}^{\text{II}}(\text{L}'(\eta^1\text{-ONO}_2))]$ (3) with concomitant formation of NO. Complexes 2 and 3 were isolated and structurally characterized. The formation of NO in the reaction was established by spin-trapping experiment. Isotopic labeling experiment revealed that the oxo transfer takes place from NO_2 to the coordinated $\eta^1\text{-ONO}$ group.



INTRODUCTION

The physiological chemistry of nitric oxide (NO) and other nitrogen oxides (NO_x) are believed to be mediated by their interactions with metal centers, especially iron and copper of metalloproteins.¹ For instance, in the state of hypoxic ischemia, nitrite (NO_2^-) ion is believed to be reduced by heme proteins to generate NO.² On the other hand, nitrogen dioxide (NO_2) is known as the key intermediate for protein tyrosine nitration.³ Hence, the reactivity of NO_2 with metal ions will be of interest with a goal of elucidating the redox transformations between various NO_x complexes. In this context, reactions of NO_2 with iron porphyrin models were described by Kurtikyan et al. Fourier transform infrared (FT-IR) optical spectroscopy and isotope labeling experiments revealed that the reaction of small amounts of NO_2 with sublimed thin layers of the [iron(II)-(Por)] complex [Por = *meso*-tetraphenylporphyrinato dianion, TPP, or *meso*-tetra-*p*-tolylporphyrinato dianion, TTP] resulted in the formation of the corresponding five-coordinate nitrito complexes $[\text{Fe}(\text{Por})(\eta^1\text{-ONO})]$.⁴ Further addition of NO_2 led to the nitrate complex $[\text{Fe}(\text{Por})(\eta^2\text{-O}_2\text{NO})]$. Another study from the same group demonstrated the reaction of NO_2 with amorphous layers of Mn(TPP) afforded the corresponding nitrate $[\text{Mn}(\text{TPP})(\eta^1\text{-ONO}_2)]$.⁵ This reaction was shown to proceed through two distinct steps: (i) initially low NO_2 pressure leads to the formation of corresponding O-nitrito complex; (ii) additional increments of NO_2 result in the nitrate analogue with the release of NO. Studies were performed with the sublimed layers of metalloporphyrins in vacuum cryostats and FTIR spectroscopy using isotopic labeling. The reaction of NO_2 with copper(II) nitrite complexes have not yet been studied, though they are relevant for copper-containing nitrite

reductases (CuNIR).⁶ Here we describe the reaction of NO_2 with a copper(II) nitrite complex.

RESULTS AND DISCUSSION

The ligand 4,6-di-*tert*-butyl-2-((2-picolyl(isopropyl)amino)methyl)phenol (LH) was prepared by refluxing a mixture of *N*-isopropyl-2-picolyamine and 2,4-di-*tert*-butylphenol in the presence of formaldehyde in methanol (Experimental Section). The formation of the ligand was confirmed by its spectral characterization and elemental analyses (Experimental Section). Mononuclear complex 1, $[\text{Cu}^{\text{II}}(\text{LH})(\text{O}_2\text{CCH}_3)_2]$, was prepared by stirring a mixture of copper(II) acetate monohydrate with equivalent quantity of LH in acetonitrile (Supporting Information). X-ray single crystal structure of complex 1 was determined. The ORTEP diagram is shown in Figure 1. The crystallographic data and important bond lengths and angles are listed in Tables 1, 2, and 3, respectively. The crystal structure reveals a distorted square pyramidal geometry around Cu(II) center in the mononuclear unit. Two acetate anions are coordinated to the metal center and balance the charge of the metal ion. The phenol moiety is coordinated to Cu(II) from an equatorial site, and Cu–O_{phenol} distance is 1.960(2) Å, which is within the range of other reported analogous complexes.⁷ The equatorial Cu–O_{acetate} distance is 1.921(3) Å, whereas the apical one is 2.534(3) Å.

In methanol, complex 1 absorbs at 470 nm (ϵ , 600 M⁻¹ cm⁻¹) and 676 nm (ϵ , 400 M⁻¹ cm⁻¹) along with strong intraligand transitions (Supporting Information). The 470 nm

Received: February 3, 2015

Published: April 30, 2015

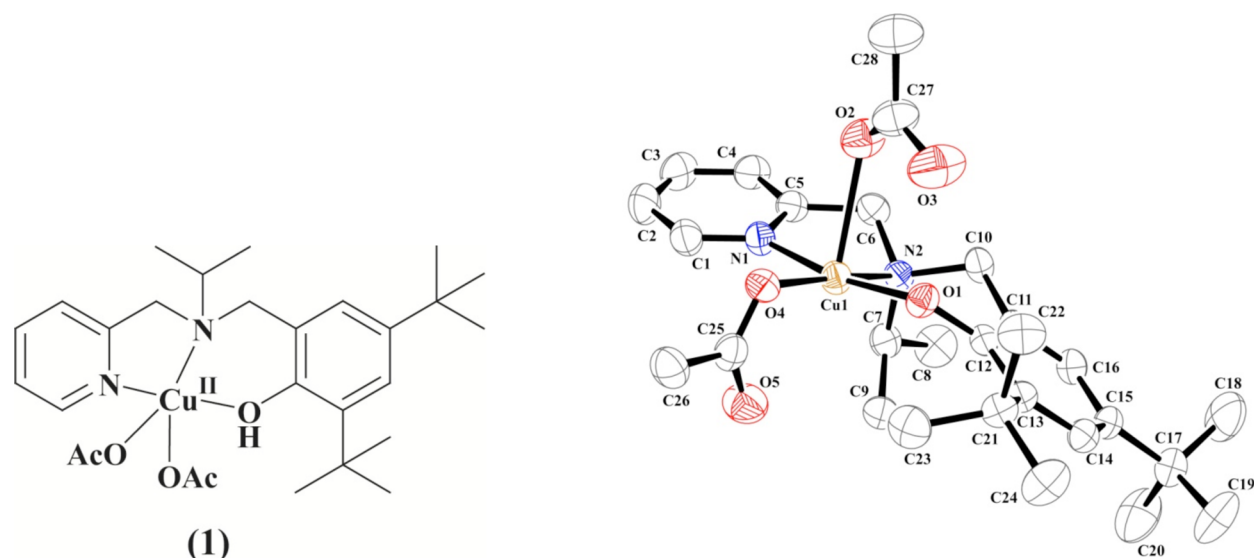


Figure 1. ORTEP diagram of complex 1 (50% thermal ellipsoid plot, hydrogen atoms are omitted for clarity).

Table 1. Crystallographic Data for Complexes 1, 2, and 3

	complex 1	complex 2	complex 3
formulas	C ₂₈ H ₄₂ CuN ₂ O ₅	C ₂₀ H ₂₆ CuN ₄ O ₅	C ₄₄ H ₅₈ Cu ₂ N ₁₀ O ₁₂
mol. wt.	550.18	466.00	1046.08
crystal system	monoclinic	orthorhombic	triclinic
space group	P2(1)/c	P2 ₁ 2 ₁ 2 ₁	P $\bar{1}$
temperature, K	296(2)	296(2)	296(2)
wavelength, Å	0.710 73	0.710 73	0.710 73
a/Å	10.116(2)	8.1018(6)	9.4692(7)
b/Å	15.428(3)	10.6660(7)	10.7391(7)
c/Å	18.573(4)	25.2840(16)	12.8212(11)
α /deg	90.00	90.00	98.363(7)
β /deg	94.603(6)	90.00	106.609(7)
γ /deg	90.00	90.00	95.160(6)
V/Å ³	2889.4(10)	2184.9(3)	1224.15(16)
Z	4	4	1
density/Mg·m ⁻³	1.265	1.417	1.419
abs. coeff./mm ⁻¹	0.793	1.038	0.938
abs. correction	none	multiscan	multiscan
F(000)	1172	972	546
total no. of reflections	4986	2440	4310
reflections, I > 2 σ (I)	2360	2105	3508
max. 2 θ /deg	25.00	25.25	25.00
ranges (h, k, l)	-11 ≤ h ≤ 11 -18 ≤ k ≤ 18 -19 ≤ l ≤ 21	-8 ≤ h ≤ 7 -10 ≤ k ≤ 10 -25 ≤ l ≤ 25	-11 ≤ h ≤ 11 -12 ≤ k ≤ 12 -15 ≤ l ≤ 11
complete to 2 θ (%)	98.2	99.9	99.8
refinement method	full-matrix least-squares on F ²	full-matrix least-squares on F ²	full-matrix least-squares on F ²
GOF (F ²)	0.885	1.073	1.241
R indices [I > 2 σ (I)]	0.0502	0.0362	0.0471
R indices (all data)	0.1097	0.0434	0.0602
largest diff. peak/hole/e Å ⁻³	0.376/-0.461	0.252/-0.352	0.344/-0.562

band is assigned as the charge transfer, and the 676 nm band is attributed to the d–d transition. The crystalline complex 1 was dissolved in methanol, and electron paramagnetic resonance (EPR) spectra were recorded at room temperature as well as at 77 K (Supporting Information). The g_{\parallel} , g_{\perp} , and A values are calculated as 2.369, 2.049, and $176 \times 10^{-4} \text{ cm}^{-1}$, respectively.

Addition of equivalent amount of NO₂ to the dry and degassed methanol solution of complex 1 resulted in the

change of color from brown to light yellow. In the UV–visible (UV–vis) spectral monitoring, both the 470 and 676 nm bands disappeared (Figure 2). EPR study revealed that the solution became EPR silent after addition of NO₂. These are attributed to the reduction of Cu(II) by NO₂ to Cu(I) (Scheme 1).⁸

In ¹H NMR spectroscopy, the broad signals of paramagnetic complex 1 became well-resolved after addition of equivalent amount of NO₂ suggesting the formation of diamagnetic

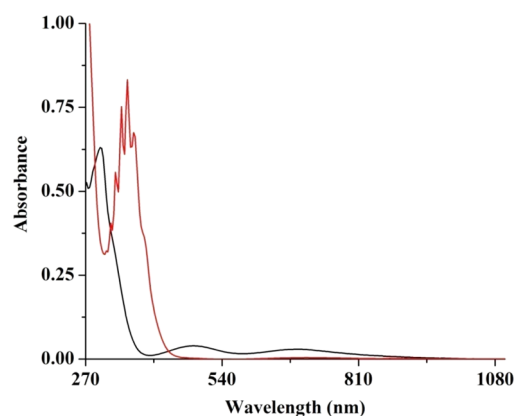
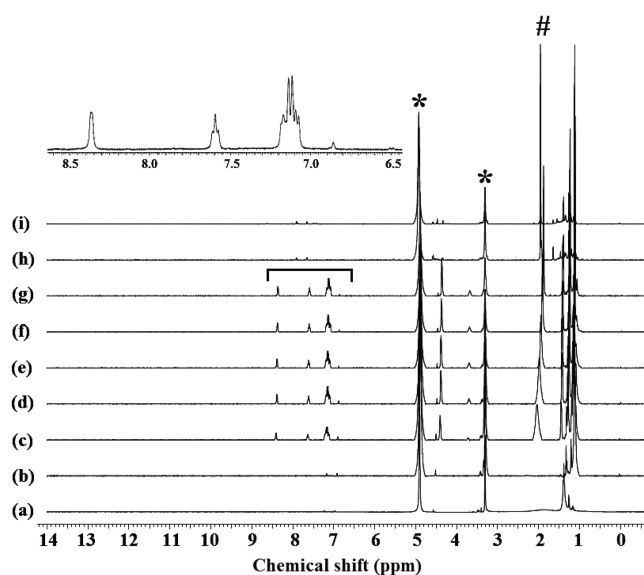
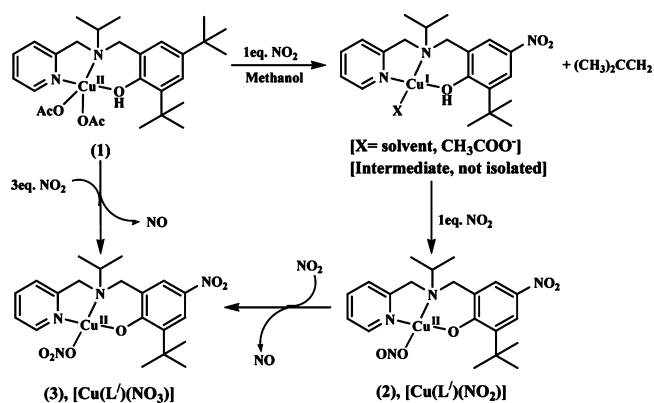
Table 2. Selected Bond Lengths (Å) of Complexes 1, 2, and 3

atoms	bond length (Å)		
	complex 1	complex 2	complex 3
Cu1–N1	2.015(3)	2.000(4)	1.965(2)
Cu1–N2	2.026(3)	2.049(4)	2.015(2)
Cu1–O1	1.960(2)	1.839(3)	1.885(2)
Cu1–O2	2.534(3)		2.015(2)
Cu1–O4	1.921(3)	1.985(4)	2.794(3)
Cu1–O5	2.786(3)	2.732(4)	
C1–N1	1.331(5)	1.339(7)	1.341(5)
C5–N1	1.338(5)	1.339(7)	1.342(4)
C1–C2	1.380(6)	1.377(8)	1.372(4)
C6–N2	1.484(4)	1.480(7)	1.494(3)
C7–N2	1.523(5)	1.513(7)	1.511(4)
C27–O2	1.193(7)		
C27–O3	1.308(6)		
N4–O2			1.299(4)
N4–O3			1.213(4)
N4–O4		1.250(7)	1.233(4)
N4–O5		1.202(7)	

Table 3. Selected Bond Angles (deg) of Complexes 1, 2, and 3

atoms	bond angles (deg)		
	complex 1	complex 2	complex 3
N1–Cu1–N2	81.4(1)	84.6(2)	84.50(9)
N1–Cu1–O1	170.0(1)	176.2(2)	171.61(9)
N1–Cu1–O2	86.2(1)		94.86(9)
N1–Cu1–O4	93.8(1)	95.2(2)	92.21(8)
N1–Cu1–O5	92.9(1)	88.8(2)	
N2–Cu1–O1	94.6(1)	91.7(2)	92.81(9)
N2–Cu1–O2	93.3(1)		179.09(9)
N2–Cu1–O4	173.1(1)	168.4(2)	130.40(8)
N2–Cu1–O5	123.0(1)	119.4(2)	
O1–Cu1–O2	84.9(1)		87.91(9)
O1–Cu1–O4	90.9(1)	88.5(2)	83.47(8)
O2–Cu1–O4	91.3(1)		50.22(8)
O4–Cu1–O5	52.0(1)	49.1(2)	
O1–Cu1–O5	96.9(1)	93.4(1)	
Cu1–O4–N4		116.0(4)	76.4(2)
Cu1–O5–N4		79.2(3)	
O2–N3–O3		122.3(5)	
O2–N4–O4			117.0(3)
O2–N4–O3			118.7(3)
Cu1–O2–Cu1			104.41(8)

species (Figure 3). The positions of ^1H NMR signals of the diamagnetic species are shifted from the positions for the free ligand. This is because of its coordination to the metal center. Earlier, it was reported that reduction of Cu(II) center of analogous complexes by NO_2 resulted in the formation of nitronium ion (NO_2^+), which in successive steps induced nitration of the phenol ring of ligand. The reaction is also associated with the simultaneous release of the tertiary butyl cation.⁸ Gas chromatography–mass spectrometry (GC-MS) analysis of the head space gas from the reaction vessel confirmed the presence of isobutylene (Supporting Information). This indicates the formation of tertiary butyl cation during the reaction. On the other hand, presence of traces of water affords tertiary butyl alcohol, as expected. In the ^1H NMR

**Figure 2.** UV-vis spectra of complex 1 (0.5 mmol) before (black trace) and after purging 1 equiv of nitrogen dioxide (red trace) in methanol at room temperature.**Scheme 1****Figure 3.** ^1H NMR spectra of complex 1 before and after purging nitrogen dioxide in CD_3OD . (a) Complex 1. (b–i) Complex 1 after the addition of 0.1, 0.2, 0.3, 0.5, 0.75, 1.0, 2.0 equiv and excess NO_2 , respectively. (inset) The aromatic region of (g) is expanded. The * marked signals are for solvent, and # marked signal indicates the formation of $(\text{CH}_3)_3\text{COD}$.

studies, the reaction of complex 1 with NO_2 was found to associate with the formation of tertiary butyl signal in the

aliphatic region (Figure 3). GC-MS of the reaction mixture also reveals the formation of tertiary butyl alcohol. Thus, it is assumed that reduction of the Cu(II) center resulted in the nitration of the phenol ring as observed earlier.⁸ This was further confirmed by isolation and characterization of the modified ligand (Experimental Section).

To the reaction mixture, addition of one more equivalent of NO₂ resulted in the appearance of a new d–d band at 660 nm along with a charge transfer band at 386 nm. The shift of charge transfer band is attributed to nitration at the phenol ring leading to the formation of modified ligand L'H.⁵ The appearance of the d–d band is presumably because of the formation of the corresponding intermediate [Cu^I–NO₂] complex, which can be considered as [Cu^{II}–NO₂[–]]. In EPR also, the four lines characteristic for Cu(II) center appeared. In ¹H NMR, the signals became broadened (Figure 3). These are in agreement with the [Cu^{II}–NO₂[–]] formulation of the intermediate complex 2. The isolation of the intermediate and structural characterization, indeed, revealed the formulation as [Cu^{II}–NO₂[–]]. The ORTEP diagram of complex 2 is shown in Figure 4. An η¹-O coordination mode of nitrite to the Cu^{II}

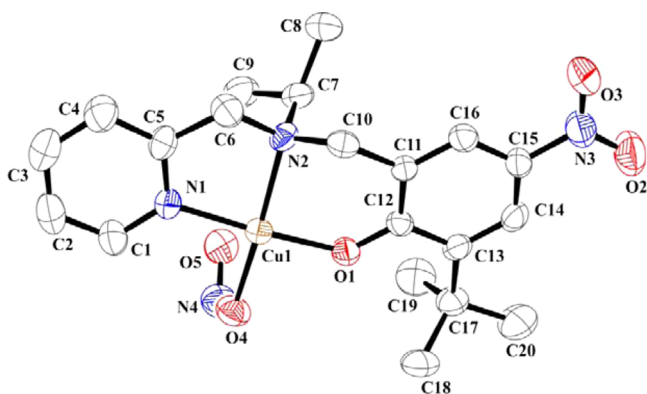


Figure 4. ORTEP diagram of complex 2 (50% thermal ellipsoid plot, hydrogen atoms are omitted for clarity).

center is observed. It is worth mentioning that in type 2 center of CuNIR and in almost all of its models, the nitrite ion binds to Cu^{II} in O,O mode.⁹ The Cu–O_{nitrito} distances are 1.985(4) and 2.732(4) Å. The Cu–O_{nitrito} bonding distances in other reported examples are ~2 Å. Cu–O–N angle is 116.0(4)°. The N–O distances are 1.250(7) and 1.202(7) Å. Note that though in comparison to other known Cu(II) nitrito complexes this binding mode is uncommon, in cases of nitrito complexes of metalloporphyrins, this is mostly observed mode.^{4,5} In FT-IR spectrum, the band at 1275 cm^{–1} is assigned to the symmetric N–O stretch, ν_s(N–O) of nitrite.⁹

Addition of NO₂ in the methanol solution of complex 2 leads to the shift of λ_{max} from 660 to 685 nm in UV–vis spectroscopy. In FT-IR studies, the nitrite stretching at 1275 cm^{–1} disappears with the appearance of a new intense stretching band at 1384 cm^{–1}. Isolation and structural characterization of the product revealed the formation of corresponding Cu(II) nitrate complex 3. The single-crystal X-ray structure of complex 3 is shown in Figure 5. In complex 3, the nitrate ion is O-coordinated in a monodentate fashion.

In MS, the peak observed at *m/z* 900.088 corresponds to the mass of nitrate bridged dicopper unit [{Cu^{II}(L')}]₂(NO₃)⁺ (Supporting Information). Expected and observed fragmentations in MS are found satisfactory (Supporting Information).

Thus, in reaction of complex 2 with NO₂ in methanol results in the oxo transfer leading to the formation of corresponding nitrate complex 3, and formation of NO is expected as side product. The release of NO was confirmed by GC-MS as well by spin trapping using iron(II)diethyldithiocarbamate complex.¹⁰

Note that addition of excess NO₂ in the methanol solution of complex 1 was found to result in the nitrate complex 3 as the final product with simultaneous release of NO. In earlier reports, Kurtikyan et al. has shown, using spectroscopic studies, that the reaction of Fe(II)(TPP) and Mn(II)(TPP) [TPP = *meso*-tetra-*p*-tolylporphyrinato dianion) with NO₂ leading to the formation of corresponding nitrate complex proceeds in two stages.^{4,5} Low NO₂ pressure and short reaction time results in NO₂ coordination to the metal center and gives O-nitrito complex of Fe(III)(TPP) and Mn(III)(TPP), respectively. This was also reported earlier by Suslick and Watson.¹¹ Subsequently, presence of additional NO₂ leads to the formation of the corresponding η¹-ONO₂ complexes, presumably with the formation of NO.^{4,5}

The conversion of complex 2 to 3, that is, O-nitrito to O-nitrate analogue in the presence of NO₂, can be envisaged by two pathways as suggested earlier by Kurtikyan et al. in case of Fe(II)(TPP) or Mn(II)(TPP) complex.^{4,5} The first mechanism would involve the attack of NO₂ to the coordinated O atom of nitrito moiety leading to the formation of O-nitrate analogue with concomitant displacement of NO from the originally coordinated nitrite (Scheme 2). Alternatively, oxygen atom transfers from free NO₂ to the nitrito N of Cu(II)–O–NO moiety (Scheme 2), which results in the analogous O-nitrate complex and NO. Though the possibility of first pathway is very rare as the homolytic cleavage of O–N bond of O-nitrito Cu(II) complex is not known, to establish the mechanism, isotope labeling experiments were performed.

If the first pathway is operating, addition scrambled NO₂^{16/18} will always result in complex 3 with single mass corresponding to [Cu(L')(¹⁶O₂N¹⁸O)] with the formation of only NO¹⁶ (Supporting Information). On the other hand, if second mechanism is operating, two equal intensity mass signals for [Cu(L')(¹⁶O₂N¹⁸O)] and [Cu(L')(N¹⁶O₃)] are expected. The mass spectrum of the reaction mixture, indeed, shows the presence of two equal intensity signals at *m/z* 902.0107 and 904.0239, respectively, for [{Cu^{II}(L')}]₂(NO₃)⁺ moiety (Supporting Information). Thus, the second pathway is suggested as the most probable one.

On the other hand, when the reaction was performed with ¹⁵NO₂, the GC-MS analysis of the head space gas reveals the presence of ¹⁵NO only (Supporting Information). This is also in accord with the proposed mechanism (Scheme 2).

The oxo transfer from NO₂ to Cu(II) nitrito complexes has not yet been observed, though found in Fe(II) and Mn(II) TPP complexes. However, only spectroscopic evidence was given for the intermediate steps. The reactivity of the present Cu(II) complex toward oxo transfer is perhaps due to the monodentate O-nitrito coordination of nitrite ion, which activates the nitrite for the reaction. This is in accord with the observations found in cases of other metal porphyrin complexes.

EXPERIMENTAL SECTION

Materials and Methods. All reagents and solvents of reagent grade were purchased from commercial sources and used as received except specified. ¹⁸O₂ was purchased from Icon Isotopes. Deoxyge-

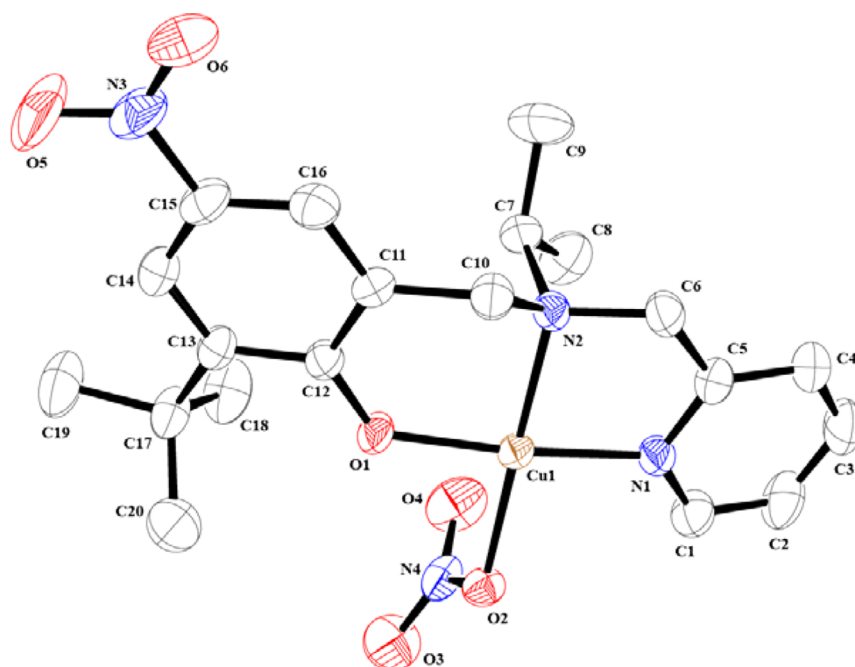
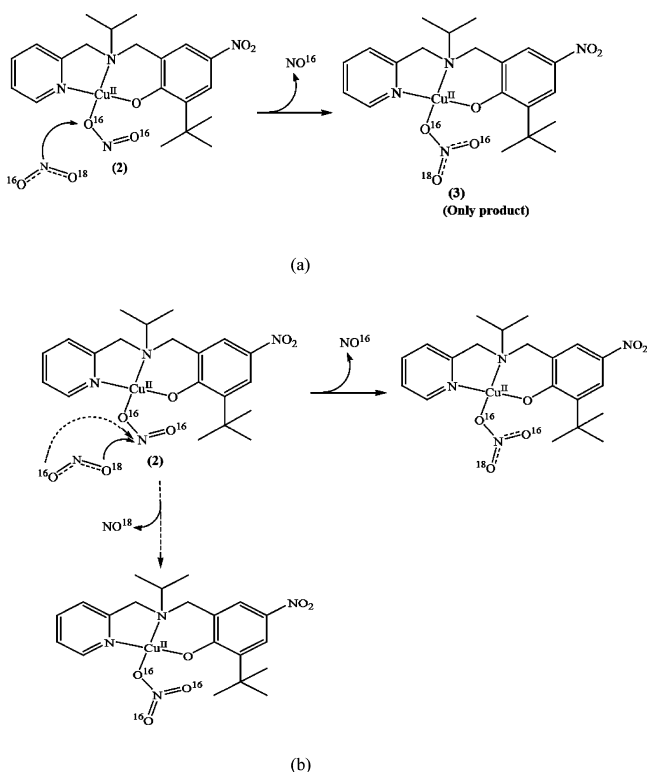


Figure 5. ORTEP diagram of complex 3 (50% thermal ellipsoid plot; hydrogen atoms and solvent molecules are omitted for clarity).

Scheme 2. Representative Scheme for the Probable Mechanism^a



^a(a) Pathway I. (b) Pathway II.

nation of the solvent and solutions was effected by repeated vacuum/purge cycles or bubbling with nitrogen or argon for 30 min. NO₂ was used from cylinder after purification using reported methods.^{4,5} ¹⁸ONO gas was prepared by the reaction of purified NO with ¹⁸O₂ in an airtight glass chamber fitted with a stoppered outlet at room temperature followed by removal of excess O₂ by passing through O₂ trap. Further purification was done following earlier reported methods

of fractional distillation.^{4,5} The isotopic enrichment of ¹⁸O in ^{16/18}O₂N is 50% as measured by GC-MS. The dilution of NO₂ was effected with argon gas using Environics Series 4040 computerized gas dilution system. UV-vis spectra were recorded on a PerkinElmer Lambda 25 UV-vis spectrophotometer. FT-IR spectra of the solid samples were taken on a PerkinElmer spectrophotometer with samples prepared as KBr pellets. Solution electrical conductivity was measured using a Systronic 305 conductivity bridge. ¹H NMR spectra were recorded in a 400 MHz Varian FT spectrometer. Chemical shifts (ppm) were referenced either with an internal standard (Me₄Si) or to the residual solvent peaks. The X-band EPR spectra were recorded on a JES-FA200 ESR spectrometer, at room temperature or at 77 K with microwave power of 0.998 mW, microwave frequency of 9.14 GHz, and modulation amplitude of 2. Elemental analyses were obtained from a PerkinElmer Series II Analyzer. The magnetic moment of complexes was measured on a Cambridge Magnetic Balance.

Single crystals were grown by slow diffusion followed by slow evaporation technique. The intensity data were collected using a Bruker SMART APEX-II CCD diffractometer, equipped with a fine focus 1.75 kW sealed tube Mo K α radiation ($\lambda = 0.71073 \text{ \AA}$) at 273(3) K, with increasing ω (width of 0.3° per frame) at a scan speed of three seconds per frame. The SMART software was used for data acquisition.¹² Data integration and reduction were undertaken with SAINT and XPREP software.¹³ Structures were solved by direct methods using SHELXS-97 and refined with full-matrix least-squares on *F*² using SHELXL-97.¹⁴ Structural illustrations were drawn with ORTEP-3 for Windows.¹⁵

Synthesis. *Ligand LH.* 2-Picolylamine (1.08 g, 10 mmol) was dissolved in 20 mL of acetone and was stirred for 2 h to give Schiff's base, after which acetone was completely removed under vacuum. Then imine was dissolved in methanol (ca. 50 mL), and 2.1 equiv of NaBH₄ was added slowly with continuous stirring. After completion of the reduction, the solvent was removed under vacuum, and to the crude mass 50 mL of water was added. The pH of the solution was maintained at ~7 pH by adding acetic acid. *N*-isopropyl-2-picolylamine was extracted from the solution by using dichloromethane (three portions each of 50 mL). Yield: 1.21 g (80%).

N-isopropyl-2-picolylamine (760 mg, 5 mmol), 2,4-di-*tert*-butylphenol (1.03 g, 5 mmol), and formalin (1.06 g of 37% solution, 13 mmol) were taken in methanol (ca. 10 mL), and the reaction mixture was refluxed for 24 h. Methanol was removed by using rotary evaporator, and after that 50 mL of water was added to the crude mixture; the

organic part was extracted by dichloromethane. Purification using alumina column chromatography yielded pure ligand **LH**. Yield: 1.19 g (65%). Elemental analysis for $C_{24}H_{36}N_2O$, calcd(%): C, 78.21; H, 9.85; N, 7.60; found(%): C, 78.28; H, 9.87; N, 7.73. FT-IR (KBr pellet) 2961, 1593, 1482, 1390, 1360, 1238, 1166, 1080 cm^{-1} . 1H NMR: (400 MHz, $CDCl_3$): δ_{ppm} : 8.50–8.49 (1H, d), 7.64–7.61 (1H, t), 7.41–7.39 (1H, d), 7.19 (1H, s), 7.14–7.11 (1H, t), 6.86 (1H, s), 3.80 (2H, s), 3.77 (2H, s), 3.12–3.09 (1H, m), 1.42 (9H, s), 1.27 (9H, s), 1.16–1.14 (6H, d). ^{13}C NMR: (400 MHz, $CDCl_3$): δ_{ppm} : 159.0, 154.4, 149.1, 140.6, 136.8, 135.6, 124.0, 123.6, 122.9, 122.3, 121.5, 55.7, 53.7, 49.6, 35.0, 34.3, 31.8, 29.8, 17.3. Mass: Calcd: (368.283), Found: 369.295 (M+1).

Complex 1. To a stirred solution of copper(II) acetate monohydrate $Cu(OAc)_2 \cdot H_2O$ (0.398 g, 2 mmol) in acetonitrile (ca. 20 mL) was added a solution of **LH** (0.740 g, 2 mmol) in chloroform (ca. 20 mL). The reaction mixture was stirred for 2 h, and then the volume was reduced under vacuum to ~ 5 mL. A layer of benzene (10 mL) was made, and the mixture was kept in freezer over night to obtain the metal complex **1** as green crystalline solid. Yield: 0.94 g (85%). Elemental analysis for $C_{28}H_{42}CuN_2O_5 \cdot CH_3CN$, calcd(%): C, 60.94; H, 7.67; N, 7.11; found(%): C, 60.99; H, 7.66; N, 7.19. UV-vis (methanol): λ_{max} (ϵ , $M^{-1} cm^{-1}$): 676 nm (400) and 470 nm (600). X-band EPR (in methanol at 77 K): g_{\parallel} , 2.369; g_{\perp} , 2.049. FT-IR (KBr pellet): 2948, 1707, 1687, 1610, 1587, 1474, 1385, 1288, 1174, 766 cm^{-1} . The complex **1** behaves as non-electrolyte in methanol solution [Λ_M ($S cm^{-1}$), 54]. The calculated magnetic moment is found to be $1.65 \mu_B$.

Complex 2. Complex **1** (550 mg, 1.0 mmol) was dissolved in dry methanol (ca. 20 mL) in a Schlenk flask fitted with a rubber septum and degassed using argon gas. To this, 2 equiv of nitrogen dioxide/argon (1:2.5 v/v) were added through a gastight syringe, and the mixture was stirred for 1/2 h. This volume of the solution was reduced under vacuum to ~ 5 mL, and a layer of diethyl ether (~ 10 mL) was made. The mixture was kept in freezer over night to afford complex **2** as greenish solid. Yield: 0.350 g ($\sim 75\%$). Elemental analysis for $C_{20}H_{26}CuN_4O_5$, calcd(%): C, 51.55; H, 5.62; N, 12.02; found(%): C, 51.61; H, 5.61; N, 12.10. UV-vis (methanol): λ_{max} (ϵ , $M^{-1} cm^{-1}$): 660 nm (240), 386 nm (17890). X-band EPR (in methanol at 77 K): g_{\parallel} , 2.367; g_{\perp} , 2.058. FT-IR (KBr pellet): 2953, 1611, 1588, 1428, 1275, 1199, 1110, 770 cm^{-1} . The complex **2** behaves as non-electrolyte in methanol solution [Λ_M ($S cm^{-1}$), 40]. The calculated magnetic moment is found to be $1.68 \mu_B$.

Complex 3. To a degassed solution of complex **1** (275 mg, 0.5 mmol) in dry methanol (ca. 10 mL), excess nitrogen dioxide gas was purged for 1 min. The resulting green colored solution was dried under vacuum to reduce its volume to ~ 5 mL. Diethyl ether (ca. 20 mL) was then added to give green precipitate of complex **3**. Product was further crystallized from acetonitrile solvent. Yield: 168 mg (70%). Elemental analysis for $C_{22}H_{29}CuN_5O_6 \cdot CH_3CN$, calcd(%): C, 51.10; H, 5.72; N, 14.89; found(%): C, 51.16; H, 5.74; N, 14.98. UV-vis (methanol): λ_{max} (ϵ , $M^{-1} cm^{-1}$): 685 nm (245), 370 nm (18 840). X-band EPR (in methanol at 77 K): g_{\parallel} , 2.362; g_{\perp} , 2.060. FT-IR (KBr pellet): 2946, 1611, 1585, 1492, 1384, 1295, 1107, 776 cm^{-1} . The complex **3** behaves as non-electrolyte in methanol solution [Λ_M ($S cm^{-1}$), 47]. The calculated magnetic moment is found to be $1.60 \mu_B$. Alternatively, complex **3** can be prepared by purging nitrogen dioxide into the methanol solution of complex **2**, also.

Isolation of Nitrated Ligand, L'H. To 30 mL of methanol solution of complex **1** (550 mg), equivalent amount of freshly prepared nitrogen dioxide/argon (1:2.5 v/v) was added through a gastight syringe. This resulting solution was allowed to stir for 10 min at room temperature. Then it was opened to air and continued stirring for 1 h. The solvent was removed under vacuum using rotavapor, and then excess aqueous Na_2S was added to give black precipitate. Solution was filtered, and modified ligand **L'H** was extracted with dichloromethane. Yield: 215 mg (60%). Elemental analyses for $C_{20}H_{27}N_3O_3$, calcd(%): C, 67.20; H, 7.61; N, 11.76; found(%): C, 67.29; H, 7.62; N, 11.87. FT-IR (in KBr): 2967, 1590, 1515, 1476, 1438, 1335, 1285, 1166, 1099, 902, 749 cm^{-1} . 1H NMR: (400 MHz, $CDCl_3$): δ_{ppm} : 8.56 (1H, s), 8.09 (1H, s), 7.83 (1H, s), 7.68–7.64 (1H, t), 7.32–7.30 (1H,

d), 7.19 (1H, s), 3.88 (2H, s), 3.81 (2H, s), 3.13–3.10 (1H, m), 1.42 (9H, s), 1.18–1.16 (6H, d). ^{13}C NMR: (400 MHz, $CDCl_3$): δ_{ppm} : 164.0, 157.5, 149.4, 139.2, 137.5, 136.9, 123.5, 123.2, 122.6, 122.5, 54.8, 53.3, 49.9, 35.1, 29.1, 17.2. Mass: Calcd: (357.205), Found: 358.173 (M+1).

Spin-Trapping Experiment to Establish the Formation of NO. Complex **2** (300 mg) was dissolved in dry and degassed methanol in a Schlenk flask attached through a rubber tubing to another flask containing a solution of $[Fe^{II}(dte)_2]$ (100 mg in 20 mL of acetonitrile). Equivalent amount of NO_2 gas (diluted using Ar gas; $NO_2:Ar$, 1:2.5 v/v) was purged in the solution of complex **2** using a gastight syringe. The mixture was stirred for 10 min. Ar gas was bubbled for 5 min through the reaction mixture to push the gas mixture into the flask containing $[Fe^{II}(dte)_2]$. X-Band EPR spectrum of this solution was then recorded to establish the presence of NO.

CONCLUSION

Thus, the reaction of Cu(II) complex $[Cu^{II}(LH)(O_2CCH_3)_2]$ (**1**) with equivalent amount of NO_2 resulted in reduction of Cu(II) to Cu(I) with concomitant nitration at the phenol ring. The in situ generated intermediate Cu(I) complex of the nitrated ligand reacts with additional equivalent of NO_2 to afford corresponding O-nitrito Cu(II) complex, $[Cu^{II}(L')(\eta^1-ONO)]$ (**2**). It was not observed earlier. Subsequent addition of NO_2 led to the corresponding O-nitrato complex $[Cu^{II}(L')(\eta^1-ONONO_2)]$ (**3**) with concomitant formation of NO. Complexes **2** and **3** were isolated and structurally characterized. Isotopic labeling experiment revealed that the oxo transfer takes place from NO_2 to the coordinated η^1-ONO group. The oxo transfer, though reported in cases of iron and manganese porphyrin complexes, was not found in literature in copper complexes.

ASSOCIATED CONTENT

Supporting Information

FT-IR, 1H and ^{13}C NMR, ESI-MS, UV-vis, X-band EPR, and GC-MS spectral data and crystallographic data in CIF files. This material is available free of charge via the Internet at <http://pubs.acs.org>.

AUTHOR INFORMATION

Corresponding Author

*E-mail: biplab@iitg.ernet.in.

Notes

The authors declare no competing financial interest.

ACKNOWLEDGMENTS

The authors thank the Department of Science and Technology (DST), India, for financial support.

REFERENCES

- (a) Cosby, K.; Partovi, K. S.; Crawford, J. H.; Patel, R. P.; Reiter, C. D.; Martyr, S.; Yang, B. K.; Wacławski, M. A.; Zalos, G.; Xu, X.; Huang, K. T.; Shields, H.; Kim-Shapiro, D. B.; Schechter, A. N.; Cannon, R. O.; Gladwin, M. T. *Nat. Med.* **2003**, *9*, 1498.
- (b) Fernandez, B. O.; Bryan, N. S.; Garcia-Saura, M. F.; Bauer, S.; Whitlock, D. R.; Ford, P. C.; Janero, D. R.; Rodriguez, J.; Ashrafián, H. *J. Biol. Chem.* **2008**, *283*, 33927. (c) Luchsinger, B. P.; Rich, E. N.; Yan, Y.; Williams, E. M.; Stampler, J. S.; Singel, D. J. *J. Inorg. Biochem.* **2005**, *99*, 912.
- (a) Averill, B. A. *Chem. Rev.* **1996**, *96*, 2951. (b) Gladwin, M. T.; Grubina, R.; Doyle, M. P. *Acc. Chem. Res.* **2009**, *42*, 157. (c) Ford, P. C. *Inorg. Chem.* **2010**, *49*, 6226.
- van der Vliet, A.; Eiserich, J. P.; Halliwell, B.; Cross, C. E. *J. Biol. Chem.* **1997**, *272*, 7617.

- (4) (a) Kurtikyan, T. S.; Hayrapetyan, V. A.; Mehrabyan, M. M.; Ford, P. C. *Inorg. Chem.* **2014**, *53*, 11948. (b) Kurtikyan, T. S.; Ford, P. C. *Angew. Chem., Int. Ed.* **2006**, *45*, 492.
- (5) Kurtikyan, T. S.; Hovhannisyan, A. A.; Gulyan, G. M.; Ford, P. C. *Inorg. Chem.* **2007**, *46*, 7024.
- (6) (a) Moura, I.; Moura, J. J. G. *Curr. Opin. Chem. Biol.* **2001**, *5*, 168. (b) Suzuki, S.; Kataoka, K.; Yamaguchi, K. *Acc. Chem. Res.* **2000**, *33*, 728.
- (7) Thomas, F.; Gellon, G.; Gautier-Luneau, I.; Saint-Aman, E.; Pierre, J. L. *Angew. Chem., Int. Ed.* **2002**, *41*, 3047.
- (8) Kumar, V.; Kalita, A.; Mondal, B. *Dalton Trans.* **2013**, *42*, 16264.
- (9) Lehnert, N.; Cornelissen; Neese, F.; Ono, T.; Noguchi, Y.; Okamoto, K.-I.; Fujisawa, K. *Inorg. Chem.* **2007**, *46*, 3916.
- (10) Melzer, M. M.; Mossin, S.; Dai, X.; Bartell, A. M.; Kapoor, P.; Meyer, K.; Warren, T. H. *Angew. Chem., Int. Ed.* **2010**, *49*, 904.
- (11) Suslick, K. S.; Watson, R. A. *Inorg. Chem.* **1991**, *30*, 912.
- (12) SMART, SAINT, and XPREP; Siemens Analytical X-ray Instruments Inc.: Madison, WI, 1995.
- (13) Sheldrick, G. M. SADABS, Software for Empirical Absorption Correction; University of Gottingen: Gottingen, Germany, 2003.
- (14) Sheldrick, G. M. SHELXS-97; University of Gottingen: Gottingen, Germany, 1997.
- (15) Farrugia, L. J. *J. Appl. Crystallogr.* **1997**, *30*, 565.